

Hadron Spectroscopy with COMPASS

Boris Grube on behalf of the COMPASS Collaboration

Physik-Department E18, Technische Universität München, James-Frank-Str., D-85748 Garching, Germany

Abstract. COMPASS is a multi-purpose fixed-target experiment at the CERN Super Proton Synchrotron aimed at studying the structure and spectrum of hadrons. One primary goal is the search for new hadronic states, in particular spin-exotic mesons and glueballs. We present recent results of partial-wave analyses of $(3\pi)^-$ and $\pi^-\eta'$ final states based on a large data set of diffractive dissociation of a 190 GeV/c π^- beam on a proton target in the squared four-momentum-transfer range $0.1 < t' < 1$ (GeV/c)². We also show first results from a partial-wave analysis of diffractive dissociation of K^- into $K^-\pi^+\pi^-$ final states are presented.

Keywords: hadron spectroscopy; light meson spectrum; strange meson spectrum; gluonic excitations; exotic mesons; hybrids.

PACS: 13.25.-k, 13.85.Hd, 14.40.Be, 14.40.Df, 14.40.Rt

INTRODUCTION

The Common Muon and Proton Apparatus for Structure and Spectroscopy (COMPASS) [1] is a fixed-target experiment at the CERN Super Proton Synchrotron (SPS). It is a two-stage high-resolution spectrometer that covers a wide range of scattering angles and particle momenta. The spectrometer is equipped with hadronic and electromagnetic calorimeters so that final states with charged as well as neutral particles can be reconstructed. A Ring Imaging Cherenkov Detector (RICH) in the first stage can be used for particle identification. It is able to separate kaons from pions up to momenta of 50 GeV/c. The target is surrounded by a Recoil Proton Detector (RPD) that measures the time of flight of the recoil protons using two scintillator barrels. COMPASS is connected to the M2 beam line of the SPS which can deliver secondary hadron beams with a momentum of up to 300 GeV/c and a maximum intensity of $5 \cdot 10^7$ s⁻¹. The negative hadron beam that was used for the analyses presented here has a momentum of 190 GeV/c and consists of 96.8 % π^- , 2.4 % K^- , and 0.8 % \bar{p} at the target. Two Cherenkov Differential counters with Achromatic Ring focus (CEDAR) upstream of the target are used to identify the incoming beam particles.

Diffractive dissociation reactions are known to exhibit a rich spectrum of produced states. In these events the beam hadron is excited to some intermediate state X via t -channel Reggeon exchange with the target. At 190 GeV/c beam energy Pomeron exchange is dominant. The X then decays into a n -body final state. The process

$$\text{beam} + \text{target} \rightarrow X + \text{recoil}, \quad X \rightarrow h_1 \dots h_n \quad (1)$$

is characterized by two kinematic variables: the square of the total center-of-mass energy, s , and the squared four-momentum transfer to the target, $t = (p_{\text{beam}} - p_X)^2$. It is customary to use the variable $t' \equiv |t| - |t|_{\text{min}}$ instead of t , where $|t|_{\text{min}}$ is the minimum value of $|t|$ for a given invariant mass of X .

$(3\pi)^-$ FINAL STATE FROM π^- DIFFRACTION

In a partial-wave analysis (PWA) of the pilot run data taken in 2004, a significant spin-exotic $J^{PC} = 1^{-+}$ resonance was found at around 1660 MeV/c² in $\pi^-\pi^+\pi^-$ final states produced in π^- diffraction on a Pb target at squared four-momentum transfers of $0.1 < t' < 1.0$ (GeV/c)² [2]. The resonance parameters are consistent with the disputed $\pi_1(1600)$ claimed in this channel by other experiments [3].

In 2008 COMPASS has acquired large data sets of diffractive dissociation of 190 GeV/c π^- on a ℓH_2 target. The trigger included a beam definition and the RPD, which ensured that the target proton stayed intact and also introduced a lower bound for t' of about 0.1 (GeV/c)². Events with charged particle trajectories outside the spectrometer acceptance and those, where the beam particle traversed the target unscattered, were vetoed. In the offline data selection events were required to have a well-defined primary interaction vertex inside the target volume. Diffractive events were

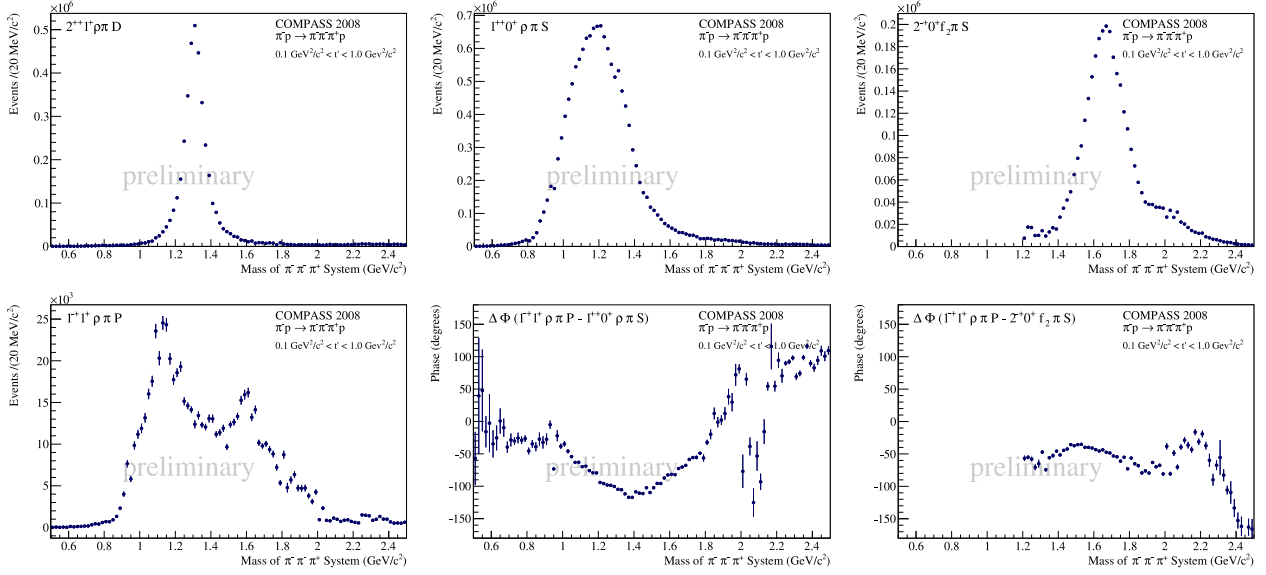


FIGURE 1. *Top row:* Intensities of major waves in $\pi^- \pi^+ \pi^-$ final state. $2^{-+} 0^+ [\rho\pi]D$ wave with $a_2(1320)$ (left), $1^{++} 0^+ [\rho\pi]S$ wave with $a_1(1260)$ (center), and $2^{-+} 0^+ [f_2\pi]S$ wave with $\pi_2(1670)$ (right). *Bottom row:* Intensity of the spin-exotic $1^{-+} 1^+ [\rho\pi]P$ wave (left) and its phase relative to the $1^{++} 0^+ [\rho\pi]S$ (center) and the $2^{-+} 0^+ [f_2\pi]S$ waves (right). (From [8])

enriched by an exclusivity cut around the nominal beam energy. After all cuts the $\pi^- \pi^+ \pi^-$ sample from the 2008 run contains $96 \cdot 10^6$ events.

In the PWA the isobar model [4] is used to decompose the decay $X^- \rightarrow \pi^- \pi^+ \pi^-$ into a chain of successive two-body decays. The X^- with quantum numbers J^{PC} and spin projection M^E is assumed to decay into a di-pion resonance, the so-called isobar, and a bachelor pion. The isobar has spin S and a relative orbital angular momentum L with respect to π^-_{bachelor} . A partial wave is thus defined by $J^{PC} M^E [\text{isobar}]L$, where $\varepsilon = \pm 1$ is the reflectivity [5].

The spin-density matrix is determined by extended maximum likelihood fits performed in $20 \text{ MeV}/c^2$ wide bins of the three-pion invariant mass m_X . In these fits no assumption is made on the produced resonances X^- other than that their production strengths are constant within a m_X bin. The PWA model includes five $\pi^+ \pi^-$ isobars [2]: $(\pi\pi)_{S\text{-wave}}$, $\rho(770)$, $f_0(980)$, $f_2(1270)$, and $\rho_3(1690)$. They were described using relativistic Breit-Wigner line shape functions including Blatt-Weisskopf barrier penetration factors [6]. For the $\pi^+ \pi^- S$ -wave we use the parametrization from [7] with the $f_0(980)$ subtracted from the elastic $\pi\pi$ amplitude and added as a separate Breit-Wigner resonance. In total the wave set consists of 52 waves plus an incoherent isotropic background wave. Mostly positive reflectivity waves are needed to describe the data which corresponds to production with natural parity exchange. A rank-two spin-density matrix was used in order to account for spin-flip and spin-non-flip amplitudes at the target vertex.

The intensity of the three dominant waves in the $\pi^- \pi^+ \pi^-$ final state, $1^{++} 0^+ [\rho\pi]S$, $2^{-+} 1^+ [\rho\pi]D$, and $2^{-+} 0^+ [f_2\pi]S$, are shown in Fig. 1, top row. They contain resonant structures that correspond to the $a_1(1260)$, $a_2(1320)$, and $\pi_2(1670)$, respectively [8]. Figure 1 bottom, left shows the intensity of the spin-exotic $1^{-+} 1^+ [\rho\pi]P$ wave. The plot nicely illustrates the unprecedented statistical accuracy due to the large data set. This wave exhibits a peak structure around $1.6 \text{ GeV}/c^2$. In this mass region a rising phase with respect to the tail of the $a_1(1260)$ in the $1^{++} 0^+ [\rho\pi]S$ wave is seen (cf. Fig. 1 bottom, center). As Fig. 1 bottom, right shows, the structure is phase locked with the $\pi_2(1670)$ in the $2^{-+} 0^+ [f_2\pi]S$ wave. This is consistent with the results obtained from a PWA of the pilot-run data taken with a Pb target [2]. The bump around $1.2 \text{ GeV}/c^2$ is still being investigated. It is unstable with respect to changes in the PWA model which hints that it might be an artifact of the analysis method. More detailed studies as well as a mass-dependent fit of the spin-density matrix are under way.

Compared to the total number of events the intensity of the spin-exotic 1^{-+} wave is on the percent level. In order to extract such small contributions reliably via PWA an excellent Monte-Carlo description of the spectrometer acceptance is required. In this regard the analysis of the isospin-partner final state $\pi^- \pi^0 \pi^0$, although having a significantly lower reconstruction efficiency, is interesting [9]. Since the reconstruction of the $\pi^- \pi^+ \pi^-$ (“charged”) and the $\pi^- \pi^0 \pi^0$ (“neutral”) final states relies on different parts of the apparatus, the results can be used for internal consistency checks. By naïve application of just isospin Clebsch-Gordan coefficients, one expects that an isovector state should decay

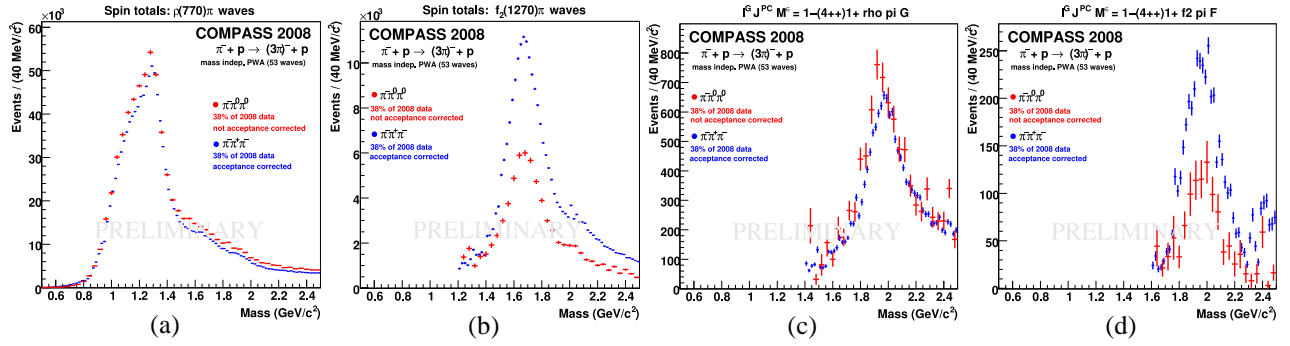


FIGURE 2. Comparison of wave intensities for $\pi^- \pi^+ \pi^-$ (blue) and $\pi^- \pi^0 \pi^0$ (red) final states: Intensity sum of all $\rho\pi$ (a) and all $f_2\pi$ waves (b). Intensity of $4^{++} 1^+ [\rho\pi]G$ (c) and $4^{++} 1^+ [f_2\pi]F$ wave (d), both with the $a_4(2040)$. (From [9])

equally into charged and neutral $(3\pi)^-$ states, if the decay proceeds via an isobar with isospin 1, whereas for an isoscalar isobar the intensity in the neutral decay channel should be half of that in the charged one. This pattern is observed in the data. Some examples are shown in Fig. 2. The two data sets are normalized to the narrow $a_2(1302)$ resonance in the $2^{++} 1^+ [\rho\pi]D$ wave. Even though no acceptance correction was applied yet to the neutral-channel data, the intensity sums of all $\rho\pi$ waves are in good agreement, whereas the intensity sums of all $f_2\pi$ waves exhibit the expected suppression factor of two in the neutral channel. This is also true for the major waves (not shown) as well as for small-intensity waves like the two 4^{++} waves shown in Fig. 2c and d. These waves contain the $a_4(2040)$ resonance and illustrate the ability of COMPASS to reconstruct resonances even in waves with percent-level intensity.

$\pi^- \eta'$ FINAL STATE FROM π^- DIFFRACTION

Other channels, where spin-exotic resonances were claimed in the past, are $\pi^- \eta$ [10, 11, 12] and $\pi^- \eta'$ [10, 13]. However, the resonant nature of the observed signals is still controversial [14]. COMPASS performed an analysis of the $\pi^- \eta'$ final state which is reconstructed from the decay chain $\eta' \rightarrow \pi^+ \pi^- \eta$, $\eta \rightarrow \gamma\gamma$. This is illustrated in Fig. 3 which shows the $\eta(548)$ peak in the $\gamma\gamma$ invariant mass spectrum. The reconstructed η are then combined with a $\pi^+ \pi^-$ pair yielding a narrow $\eta'(958)$ peak in the respective invariant mass distribution. The final $\pi^- \eta'$ invariant mass spectrum contains 35 000 events and exhibits a peak from the $a_2(1320)$ resonance.

The performed PWA [15] follows previous analyses and includes S , P , and D waves with $M \leq 1$ and both natural and unnatural parity exchange. In addition a $4^{++} 1^+$ and a background wave were included. The top row of Fig. 4 shows the intensities of the major waves. The $2^{++} 1^+$ (D_+) wave exhibits a peak of the $a_2(1320)$ and the $4^{++} 1^+$ (G_+) wave a clear signal of the $a_4(2040)$. The most intense wave, however, is the spin-exotic $1^{-+} 1^+$ (P_+) wave which has a broad structure around $1.6 \text{ GeV}/c^2$, consistent with previous experiments. The P_+ wave shows slow phase motion with respect to the D_+ wave in the $1.6 \text{ GeV}/c^2$ mass region (see Fig. 4 bottom, left). A mass-dependent fit of the spin-density matrix is work in progress.

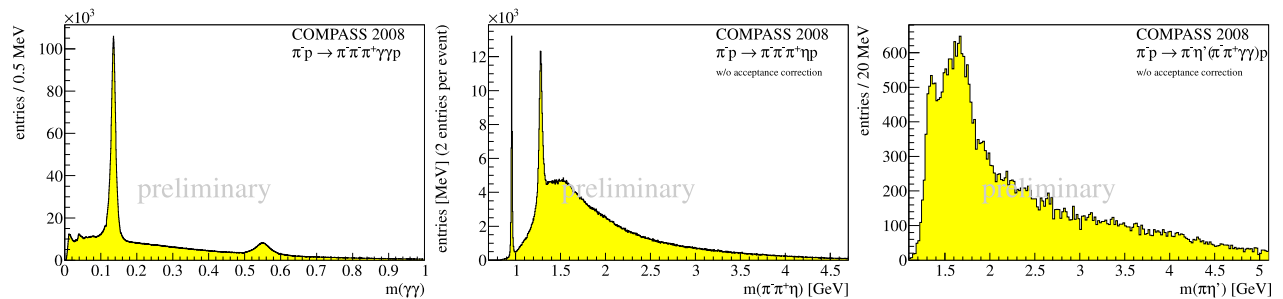


FIGURE 3. Left: $\gamma\gamma$ invariant mass distribution with the π^0 and η peaks for events with three charged tracks. Center: $\pi^+ \pi^- \eta$ invariant mass spectrum. Right: $\pi^- \eta'$ invariant mass distribution with visible $a_2(1320)$ peak. (From [15])

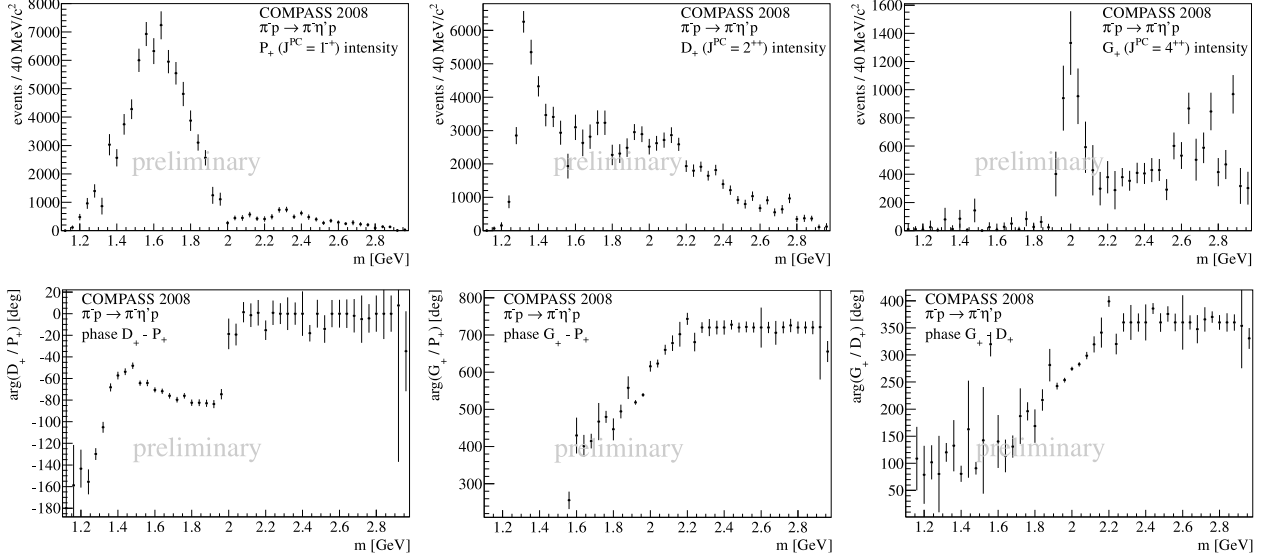


FIGURE 4. Top row: Intensities of major waves in $\pi^- \eta'$ final state. Spin-exotic $1^{++} 1^+$ (P_+) wave (left), $2^{++} 1^+$ (D_+) wave with $a_2(1320)$ (center), and $4^{++} 1^+$ (G_+) wave with $a_4(2040)$ (right). Bottom row: Relative phases of major waves in $\pi^- \eta'$ final state. $D_+ - P_+$ (left), $G_+ - P_+$ (center), and $G_+ - D_+$ (right). (From [15])

$K^- \pi^+ \pi^-$ FINAL STATE FROM K^- DIFFRACTION

Although there are no spin-exotic strange mesons, because these states are not G - or C -parity eigenstates, the spectrum of strange mesons is still interesting as it contains many states that need confirmation. There are also open questions about the interpretation of some states. Since most of the available data are from the 70s and 80s, COMPASS takes the opportunity to remeasure some final states with a state-of-the-art apparatus. An interesting channel is the $K^- \pi^+ \pi^-$ final state which was studied by several experiments in the past [16]. The measurement [17] exploits the fact that the negative hadron beam of the M2 beam line contains a 2.4 % admixture of K^- . These beam kaons were tagged by two CEDAR detectors located 30 m upstream of the target. The final-state kaons were identified using the RICH detector. After all cuts a sample of 270 000 $K^- \pi^+ \pi^-$ events was obtained. Figure 5 shows the $\pi^+ \pi^-$ invariant mass spectrum which exhibits structures from $\rho(770)$, $f_0(980)$, and $f_2(1270)$. The corresponding $\pi^+ K^-$ spectrum shows peaks from $K^*(892)$ and $K_2^*(1430)$. Also the $m_{K^- \pi^+ \pi^-}$ distribution shows significant structures.

A PWA using a model with 19 waves plus a background wave together with a rank-2 spin-density matrix was performed in 20 MeV/c² wide mass bins. Some of the most prominent waves are shown in Fig. 6. A clear $K_2^*(1430)$ peak is seen in the $2^+ 1^+ [K^*(892)\pi]D$ wave. The $1^+ 0^+ [K^*(892)\pi]S$ wave shows two peaks that probably belong to the $K_1(1270)$ and the $K_1(1400)$. As expected the $K_1(1400)$ peak is absent in the corresponding $1^+ 0^+ [\rho K]S$ wave (not

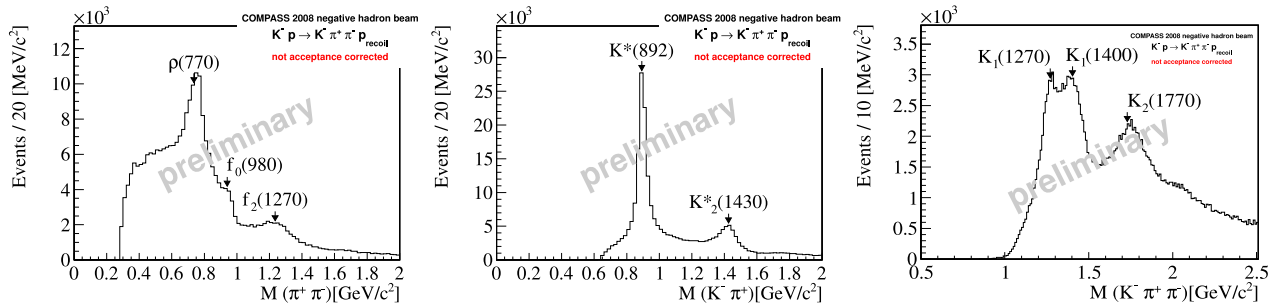


FIGURE 5. Left: $\pi^+ \pi^-$ invariant mass distribution for $K^- \pi^+ \pi^-$ events. Center: respective $\pi^+ K^-$ invariant mass spectrum. Right: $K^- \pi^+ \pi^-$ invariant mass distribution. (From [17])

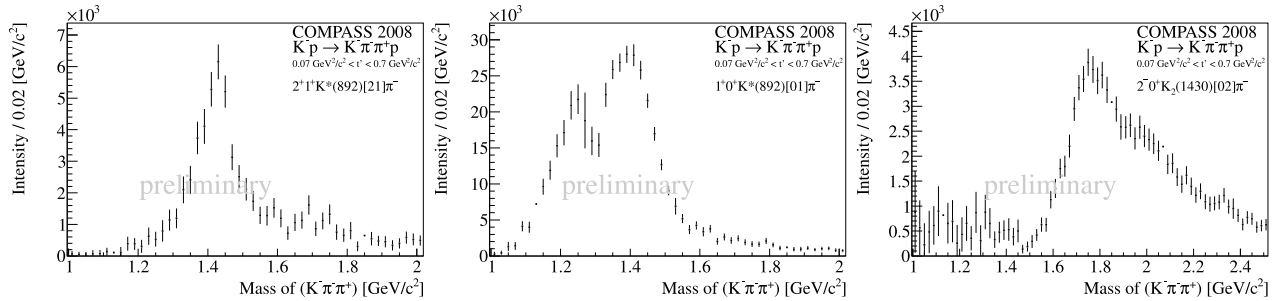


FIGURE 6. Intensities of some dominant waves in the $K^- \pi^+ \pi^-$ final state: $2^+ 1^+ [K^*(892)\pi]D$ wave (left), $1^+ 0^+ [K^*(892)\pi]S$ wave (center), and $2^- 0^+ [K_2^*(1430)\pi]S$ wave (right). (From [17])

shown). Similarly the broad structure in the $2^- 0^+ [K_2^*(1430)\pi]S$ wave, which could be due to $K_2(1770)$ and $K_2(1820)$, becomes narrower in the $2^- 0^+ [f_2(1270)K]S$ wave (not shown). More information on these and other states will be extracted by fitting the mass dependence of the spin-density matrix.

CONCLUSIONS

First partial-wave analyses of the large data set of diffractive dissociation events that COMPASS has collected show interesting results in various channels. Structures around $1.6 \text{ GeV}/c^2$ are observed in spin-exotic $J^{PC} = 1^{-+}$ waves in the $\rho\pi$ and the $\pi\eta'$ decay channels. The resonant nature of these bumps, however, still has to be verified by mass-dependent fits. The same is true for some structures seen in the $K^- \pi^+ \pi^-$ final state. With further improved analyses COMPASS will make a significant contribution to the study of the light-quark meson spectrum.

ACKNOWLEDGMENTS

This work is supported by the German BMBF, the Maier-Leibnitz-Labor der LMU und TU München, the DFG Cluster of Excellence *Origin and Structure of the Universe*, and CERN-RFBR grant 08-02-91009.

REFERENCES

1. P. Abbon *et al.*, Nucl. Instrum. Methods **A577**, 455–518 (2007); M. Alekseev *et al.*, “The COMPASS 2008 Spectrometer” to be submitted to Nucl. Instrum. Methods **A** (2011).
2. A. Alekseev *et al.*, Phys. Rev. Lett. **104**, 241803 (2010).
3. G. S. Adams *et al.*, Phys. Rev. Lett. **81**, 5760 (1998); Y. Khokhlov, Nucl. Phys. **A663**, 596 (2000); S. U. Chung *et al.*, Phys. Rev. **D65**, 072001 (2002).
4. J. D. Hansen *et al.*, Nucl. Phys. **B81**, 403 (1974).
5. S. U. Chung and T. L. Trueman, Phys. Rev. **D11**, 633 (1975).
6. F. von Hippel and C. Quigg, Phys. Rev. **D5**, 624 (1972).
7. D.V. Amelin *et al.*, Phys. Lett. **B356**, 595 (1995).
8. F. Haas, to appear in Proceedings of Hadron2011, eConf (2011).
9. F. Nerling, to appear in Proceedings of Hadron2011, eConf (2011).
10. G. Beladidze *et al.*, Phys. Lett. **B313**, 276–282 (1993).
11. D. Thompson *et al.*, Phys. Rev. Lett. **79**, 1630–1633 (1997).
12. A. Abele *et al.*, Phys. Lett. **B423**, 175–184 (1998).
13. E. I. Ivanov *et al.*, Phys. Rev. Lett. **86**, 3977–3980 (2001).
14. A. Szczepaniak, M. Swat, A. Dzierba, and S. Teige, Phys. Rev. Lett. **91**, 092002 (2003).
15. T. Schlüter, to appear in Proceedings of Hadron2011, eConf (2011).
16. G. W. Brandenburg *et al.*, Nucl. Phys. B, vol. 86, no. 3, pp. 381–402, 1975; Y. M. Antipov *et al.*, Nucl. Phys. **B86**, 381–402 (1975); C. Daum *et al.*, Nucl. Phys. **B186**, 205–218 (1981); H. Guler *et al.*, Phys. Rev. **D83**, 032005 (2011).
17. P. K. Jasinski, to appear in Proceedings of Hadron2011, eConf (2011).